IEEE Photonics Journal
An IEEE Photonics Society Publication

Open Access

Improvement on Direct Modulation Responses and Stability by Partially Corrugated Gratings Based DFB Lasers With Passive Feedback

Volume 13, Number 1, February 2021

Siti Sulikhah, *Member, IEEE*
San Liang Lee, *Senior Member, IEEE*
Hen Wai Tsao, *Senior Member, IEEE*

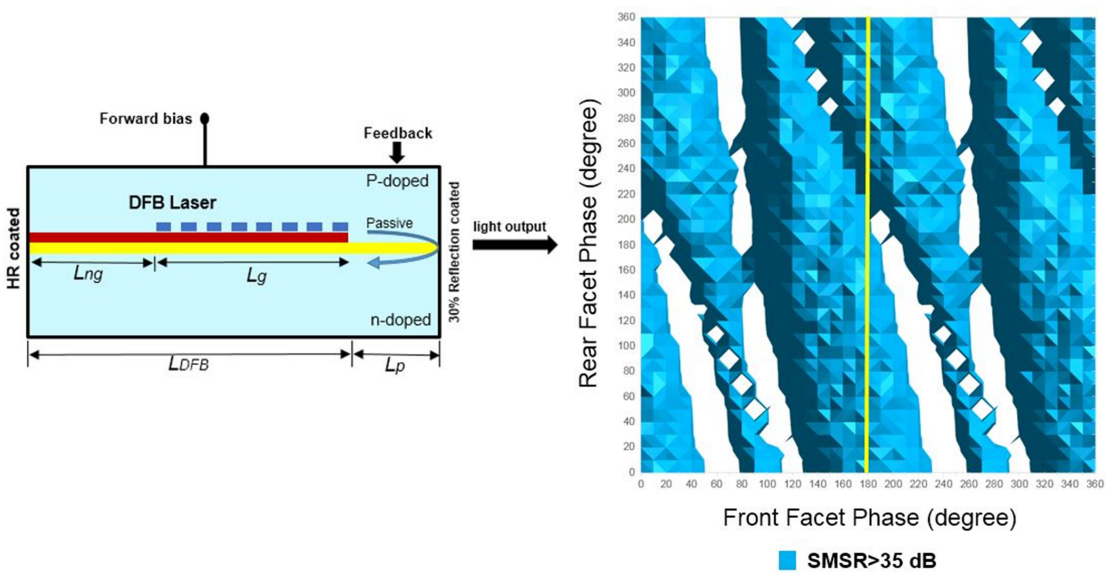

DOI: 10.1109/JPHOT.2021.3056241

Improvement on Direct Modulation Responses and Stability by Partially Corrugated Gratings Based DFB Lasers With Passive Feedback

Siti Sulikhah,[1] ***Member, IEEE***,
San Liang Lee,[1] ***Senior Member, IEEE***,
and Hen Wai Tsao,[2] ***Senior Member, IEEE***

[1]Department of Electronic and Computer Engineering, National Taiwan University of Science and Technology, Taipei 10607, Taiwan
[2]Department of Electrical Engineering, National Taiwan University, Taipei 10607, Taiwan

DOI:10.1109/JPHOT.2021.3056241

Manuscript received December 17, 2020; revised January 26, 2021; accepted January 28, 2021. Date of publication February 2, 2021; date of current version February 22, 2021. This work was supported by the Ministry of Science and Technology (MOST), Taiwan through Research and Implementation of Key Technologies for Lithographic Three-Dimensional Laser Scanning Wafers Project under Grant MOST 108-2622-E-011-001-CC1. Corresponding author: San Liang Lee (e-mail: sllee@mail.ntust.edu.tw).

Abstract: DFB lasers with ultrashort cavities or integrated DFB lasers with passive waveguide reflectors are frequently proposed to realize directly modulated lasers (DMLs) for carrying ultrahigh data rate signals. The former suffers from poor heatsink and laser cleavage yield, while the single-mode stability of the latter scheme is seldom addressed. The mode selection and device performance of a DFB laser is well known to be very sensitive to the facet reflection and external optical feedback. The DFB lasers with partial corrugated gratings and passive feedback (PCG-PFL) are proposed here to overcome the challenging issues for the aforementioned two schemes. With PCG structure, the DFB lasers can maintain high single-mode yield (SMY) even with a high-reflection-coating on the rear facet and strong reflection from the integrated passive section. This provides the robustness in applying the integrated passive reflector to reshape the modulation response or to enhance the 3-dB bandwidth by using the photon-photon resonance (PPR) effect. By designing the PCG-PFL to have 150-μm long laser section, 50-μm long passive section, and 30% front-facet reflectivity, it can have about 86% of SMY, reduced resonant peak in the intensity modulation response, and reduced waveform overshoot and undershoot for transmitting 56-Gbaud/s PAM-4 signals. By using a longer passive reflector, enhanced bandwidth can be achieved by the PPR effect.

Index Terms: Directly modulated laser (DML), stability, passive feedback, partially corrugated grating, PAM-4 modulation, single-mode yield, photon-photon resonance.

1. Introduction

High-speed light sources are the key light sources for enabling high-capacity optical networking, and their applications are expanding from long distance transmission to optical interconnects for data centers. Directly modulated lasers (DMLs), electro-absorption modulated lasers (EMLs), and a combination of off-chip laser sources and silicon photonic optical modulators are among the

favorites for transmitting optical data of >50-Gb/s data rates. DMLs have the merits of low cost and low power consumption, which is especially important for inside data center applications.

The distributed feedback (DFB) lasers has the potential to provide the required bandwidth for carrying >100-Gb/s signals [1]–[3].To achieve 100-Gb/s per channel transmission with 4-level pulse amplitude modulation (PAM-4), the required transmitter bandwidth is 31-GHz [4], which has been demonstrated by several groups for direct modulation of DFB lasers. The techniques to accomplish ultrahigh-speed modulation for DMLs can be classified into two categories: pure carrier-photon resonance (CPR) type and photon-assisted type. The latter includes the schemes using photon-photon resonance (PPR) and detuned loading mechanisms [5].

The modulation bandwidth of CPR type lasers can be enhanced by optimizing the laser geometry and materials to shorten the laser cavity, increase the confinement factor, and raise the differential gain of multiple quantum well (MQW) structures. The modulation bandwidth can also be enhanced by the photon-assisted effect through optical injection locking (OIL), integrated grating reflectors, and integrated passive reflectors [6]–[9]. As specific examples, some research groups demonstrate the use of shorter-cavity DFB laser to achieve high modulation bandwidth, but it suffers from the cleavage yield and poor heatsink issues [10], [11]. One solution to solve the issues with a short-cavity DFB laser is to add a passive section of which the end facet is applied with an anti-reflection (AR) coating. On the other hand, DFB lasers with uniform grating (UG-DFB) and passive feedback have been reported for modulation speed up to 40-Gb/s [12]–[14]. The integrated DFB lasers with external grating feedback were demonstrated to enhance the modulation bandwidth to >50-GHz and transmit >100-Gb/s 4-level PAM-4 signals [15]–[17]. Recently, NTT presented the DML with >100-GHz bandwidth, based on membrane-III-V-on-SiC technology and a PPR-supporting cavity design [18]–[19].

Though DFB lasers with integrated passive section and reflectors have been demonstrated by several groups to enhance modulation bandwidth, the effects of the external-cavity reflection on the laser mode stability were seldom addressed. It is well known that a DFB laser is very sensitive to the facet phase fluctuation, especially when the laser end facets are not coated with AR coatings. In practice, a high-reflection (HR) coating on the rear facet is favored to increase the optical output power from the front facet. High power is essential for ultrahigh data rate operation. The HR coating will degrade the single-mode yield of DFB lasers even when quarter-wavelength or multiple phase shifts are incorporated into the grating structure. When a passive section with reflector is added to the laser structure in order to enhance the modulation bandwidth, the tuning of feedback phase is very likely to affect the mode selectivity of DFB lasers, complicate the operation of the integrated laser structure, and degrade the stability of the operation condition.

We proposed here the DFB laser with partial corrugated gratings (PCG) for integration with a passive section with partial feedback to enhance the modulation bandwidth and/or the modulation response for transmitting >100-Gb/s signals. The focus is the mode stability under the change in the phase of the partial feedback. For demonstration, we design and optimize the PCG-DFB with passive feedback laser (PCG-PFL) to reduce the relative intensity noise (RIN) and resonant peak in the modulation response. These two effects can enhance the waveform and eye opening for high-speed PAM modulation. PCG structures are incorporated into the laser structure in order to maintain the single-wavelength yield under strong reflection from the passive section [20]–[22].

2. Device Structure and Stability

The PCG-DFB lasers have been demonstrated to provide good SMSR and high-resistance to external optical feedback [23], [24]. It can be realized with simple holographic exposure without the use of phase-shift gratings that are fabricated by e-beam writing schemes. In our prior work, the integrated EMLs with PCG-DFB was verified to have high single-mode yield under the influence of residual facet reflection from the modulator side.

To further increase the bandwidth for transmitting PAM-4 signals of 50-Gbaud/s or beyond data rates, the laser length needs to be shortened. Besides the challenges in laser cleavage of short-cavity lasers, such a high-speed laser is subject to the gain saturation and thermal heating.

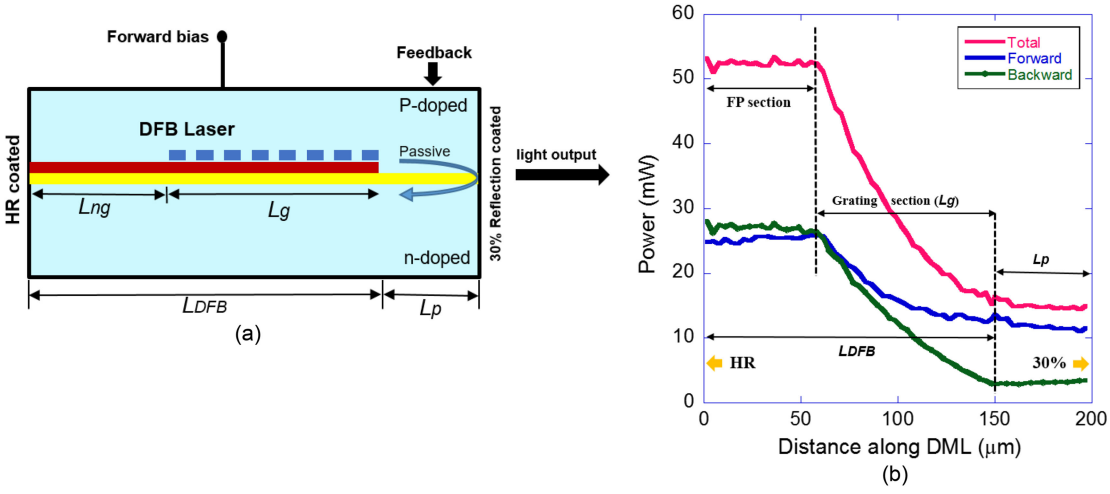

Fig. 1. (a) Schematic of PCG-DFB laser having passive feedback. (b) Longitudinal power distribution of: forward propagation, backward propagation, and total field of the PCG-PFL in static condition with L_{DFB} of 150-μm and $L_p = 50$-μm. The HR facet phase was set to 0° and front facet = 180°.

Combining a short-cavity PCG-DFB and a passive section can provide many advantages over different device configurations. Firstly, a short-cavity PCG active section plus an integrated AR-coated passive section can achieve both large bandwidth, good thermal conduction, and stable operation condition even if some residual reflection exists at the AR-coated facet. Secondly, the PCG-DFB can be integrated with a short passive reflector for reshaping the modulation response, which is good for PAM-4 modulation. Thirdly, a PCG-DFB laser can be integrated with a mid-length passive reflector to enhance the modulation bandwidth by the PPR effect. Here, we refer these three types of laser sources as PCG-DFB lasers having partial feedback (PCG-PFL). The other configurations include the integration with external grating based detuned loading filter or multiple laser cavities that will not be addressed here. For the first type of PCG-PFL, our modeling can account for the residual facet reflection of AR coating. The choice of PCG-DFB lasers over the conventional DFB lasers with uniform grating (UG) or phase-shifted gratings can avoid the necessity of fabrication with expensive and low-throughput e-beam writers in addition to its immunity to external feedback [25]–[27].

Fig. 1(a) shows the schematic diagram of a PCG-PFL, which includes three-sections: an active region without grating of length L_{ng}, an active region with corrugated grating of length L_g, and a passive feedback section of length L_p. The PCG-DFB laser length is L_{DFB} ($= L_{ng} + L_g$) and the total laser length is L ($= L_{DFB} + L_p$). The device parameters for MQWs and waveguide parameters are chosen to make the laser to have >30-GHz bandwidth as reported in the literature [28]. The rear facet (laser end) of the PCG-PFL is coated with HR film of 90% reflectivity. The HR coating on the PCG-DFB rear facet can increase the slope efficiency of the laser output but also create a harsh condition for the laser cavity to maintain a stable operation with facet phase fluctuation and optical feedback. This can test the robustness of the laser structure. A similar DFB laser with passive feedback is reported in [29] where a tuned passive feedback section is integrated on the rear end of a UG-DFB to provide PPR modulation bandwidth enhancement.

Fig. 1(b) depicts the longitudinal power distribution inside a PCG-PFL under static condition with L_{DFB} of 150-μm and $L_p = 50$-μm. The device parameters and simulation methodology will be described in the next section. From the power distribution, the PCG-DFB region of a PCG-PFL laser can be regarded as an FP laser with an active grating reflector. This model can help to explain why a PCG-DFB is less sensitive to the facet phase fluctuation of the HR coating and has a larger resistance to external optical feedback [20].

The optical feedback effects on the laser dynamics for external cavity or integrated multiple sections have been well investigated [30]–[33]. Our goal here is to discuss the advantages of using PCG-PFLs as ultra-high-speed lasers. The PCG-DFB laser of a PCG-PFL can be modeled as two active sections with and without gratings. To analyze the PCG-PFL dynamics under external optical feedback, intensive efforts in deriving the dynamic mirror loss, Bragg deviation, and fluctuation in the photon and carrier densities due to the optical feedback needs to be carried out [20], [21]. Here, we adopt the simple criterion for mode stability of a single-frequency semiconductor laser [31], [33]. The stability of a laser with external cavity can be maintained if [34]

$$C = K_f \tau_{ext}\sqrt{1+\alpha^2} \approx \sqrt{R_f} e^{-\alpha_p L_p} \frac{\tau_{ext}}{\tau_L}\sqrt{1+\alpha^2} < 1 \quad (1)$$

where τ_{ext} is the round-trip time of the optical feedback, α is the linewidth enhancement factor, and K_f is the normalized reflected field injection rate per round-trip time of the laser cavity [34], which is related to R_f: the reflectivity at the front facet, τ_L: the round-trip time of the PCG-DFB laser cavity, and the intrinsic loss coefficient (α_p) and length (L_p) of the passive section. C is the feedback coefficient that represents the level of feedback effect on the laser operation [34]. The interface between the active grating and passive section is assumed to be of no loss and reflection for simplicity. When the inequality in (1) holds, multiple mode solutions will not exist, so the laser can be operated at the stable single-mode condition. The partial reflection of the passive section will still affect the threshold current, lasing wavelength, and other laser characteristics.

The laser structure discussed here corresponds to the short external cavity case where τ_L is smaller than the relaxation resonance period [14]. For the targeted high-speed lasers, the relaxation resonance period can be as short as 25-ps [17], [18], but τ_L is typically less than 10-ps for this type of lasers. From (1), the laser may turn unstable (C $>$ 1) and cause self-pulsations for a longer passive section or larger facet reflectivity.

The design of a PFL needs to account for all feedback mechanisms, which take place throughout the laser cavity. By using PCG-DFB structures, the measures to cope with the performance improvement by optical feedback for PFL are more robust. Even with strong feedback, it is possible to operate the laser at a single longitudinal lasing mode with an excellent single-mode yield without using a phase control to stabilize the mode. However, the laser dynamic can be perturbed by the facet reflection, which will be determined by the feedback strength and phase of the reflected field [35]. We investigate the performance of a PCG-DFB laser with an integrated reflective passive section against the rear/front facet phase fluctuation. The goal is to provide a robust device structure for applying the passive feedback to enhance the modulation response of a high-speed DML.

3. Device Simulation Approach

The static and dynamic responses of PFLs are analyzed to test the laser performance, i.e., single-mode yield, RIN characteristics, intensity modulation (IM) responses, and eye diagrams for non-return-to-zero (NRZ) or PAM-4 modulation, against rear and front facet phase variations. In addition to the mode stability, the feasibility of high-speed operation of PFLs relies on a reduced overshoot and undershoot that are correlated with the relaxation resonance in the laser cavity. Since the passive reflection can reshape the frequency response of the laser, the modulated output waveforms can be enhanced. Thus, a PCG-PFL can generate a large eye opening. For a conventional DFB laser, the interaction between photons and carriers under optical feedback could cause severe wavelength and waveform fluctuation, which is critical in the signal transition, especially for carrying PAM-4 signals.

The responses of the PCG-PFL is analyzed with VPIcomponentMaker Photonics Circuits tool, which works based on the time-dependent transmission line laser model (TLLM) [36]. The TLLM could be applied to a single-section or multi-section semiconductor devices with a built-in optical waveguide made from MQW active medium. This model permits the simulation of device structures

TABLE I
List of Device Parameters

Parameter	Value	Unit	Parameter	Value	Unit
DFB section length	150	μm	Transparent carrier density	2.5×10^{24}	$1/m^3$
Active region width	1.5	μm	Linewidth enhancement factor	3	-
Active region depth of MQW	0.06	μm	Rear facet reflectivity	90	%
Confinement factor of MQW	0.12	-	**Passive Section Model** [43]		
Grating coupling strength, κ	8000	m^{-1}	Passive section length	50	μm
Linear gain coefficient	12×10^{-20}	m^2	Confinement factor of passive section	0.6	-
Internal loss	30	cm^{-1}	Internal loss of passive section	30	cm^{-1}
Group index	3.73	-	Front facet reflectivity	30	%

with different grating types and waveguide parameters like PFLs. In addition to the threshold current, output power, and side-mode suppression ratio (SMSR), this tool can also simulate the modulation response, linewidth, and RIN of a laser [37]–[39]. The TLLM simulation model accounts for the forward and backward propagating waves inside the laser as well as the spatial dependency of the device parameters by dividing the device into multiple longitudinal sections. Therefore, it can account for the spatial hole burning effect from non-uniform carrier and light distribution inside the laser cavity. In addition, the scattering of light inside each TLLM section is considered as the result of the interactions between the optical and electronic subsystems for different types of device sections. Self-pulsation mechanism is also included in the simulation model [40], [41].

To justify the performance enhancement, we first compare single-mode yield (SMY) between a UG-PFL and a PCG-PFL. The SMY of PCG-PFLs is then evaluated for different extent of reflectivity and grating coupling coefficient. The RIN, IM response, and output waveforms are simulated and compared for PCG-DFB lasers with and without passive feedback. The SMY is defined as the percentage of rear and front phases that the laser can have >35-dB SMSR for single-mode lasers. The front phase refers to the phase of the partial reflection from the passive section.

4. Simulation Results

Definitions and values of the key laser parameters used in analyzing the dynamic performance of directly modulated PFLs are summarized in Table 1. A high-speed DML typically requires a larger differential gain which can be achieved with proper MQW design by optimizing the material composition and number of wells. For example, by using 20-well InGaAlAs–InGaAsP strain-compensated MQWs, $>14\times10^{-20}$ m^2 differential gain can be obtained [42]. The TLLM modeling adopted here does not include the simulation of gain spectrum of the MQW. Instead, a differential gain coefficient is assumed in the simulation.

The PCG-PFL with short ($50-\mu$m) passive section will be investigated first. For such a short passive reflector, the PPR frequency is beyond 100-GHz, so the influence of optical feedback on the modulation response can be clearly observed. The PPR effect will be demonstrated with a PCG-PFL with a longer (200-μm) passive reflector.

The laser is operating at 1550-nm wavelength with DC current of 40-mA. For the PCG-PFL, its PCG-DFB section has a grating length about 60% of L_{DFB}, which provides a good 3-dB bandwidth and reflection resistance [23], [24]. Fig. 1(b) shows the longitudinal power distribution of PCG-PFL at stable and good SMSR condition.

The SMY is analyzed for PCG-PFLs with various rear and front phases ranging from 0 to 2π. When $L_g = L_{DFB}$, PCG-PFL becomes UG-PFL. For eye-diagram analyses, a 4^{th}-order low pass filter (LPF) is set at transmitter side. The system performance is evaluated by transmitting 2^{17}-1 pseudorandom bit sequence (PRBS) data stream with a transmitter LPF bandwidth of 75% data rate. Meanwhile, a 25-GHz electrical LPF is used in the receiver [44]–[46].

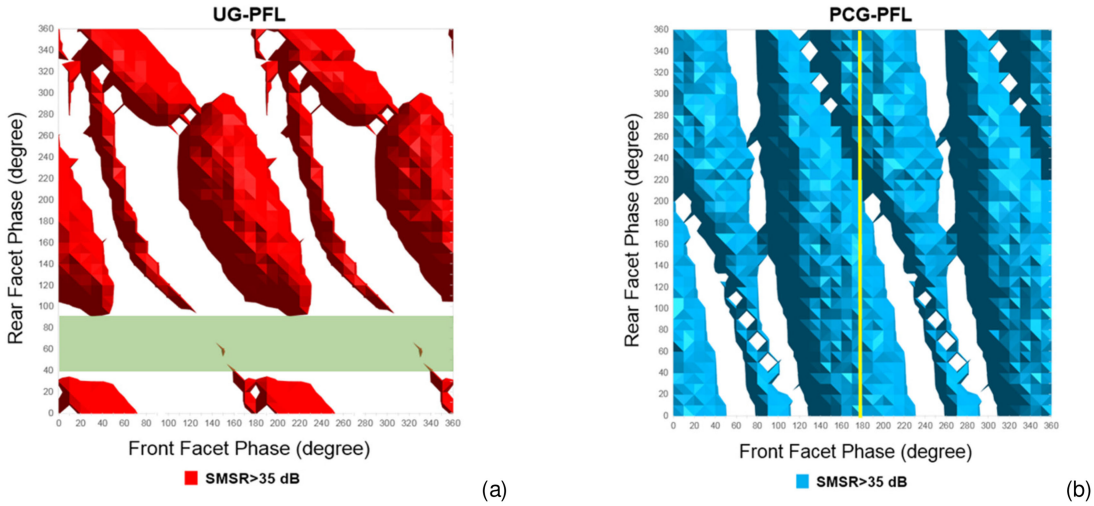

Fig. 2. Comparison of SMSR between (a) UG-PFL and (b) PCG-PFL with phase variation from 0 to 2π for the rear HR coating and front facets.

4.1 Comparisons Between UG-PFL and PCG-PFL

The simulated SMSR at different facet phases for the UG-PFL and PCG-PFL with a 50-μm long passive section is depicted in Fig. 2, which shows clear difference between the two contour maps for UG- and PCG-PFLs in varying the rear facet and front facet phases. The colored region represents where the SMSR of the PFL output exceeds 35-dB. The single-mode yield is 46.6% and 85.98% for UG-PFL and PCG-PFL, respectively. The results verify that the PCG-PFL can maintain a more stable single-mode operation compared to UG-PFL since the latter is relatively sensitive to the change in both facet phases. The better resistance to external feedback of a PCG-PFL is attributed to the releasing of the reflection-induced phase fluctuation to the whole non-corrugated section of a PCG-DFB laser [24]. This effect helps to stabilize the laser performance under the influence of optical reflection, so a much better SMY could be achieved. This result is consistent with the previous findings of better resistance to external reflection for PCG-DFBs [23], [24]. That is, even with a HR-coated facet, it is relatively easy to locate the operation condition for using the integrated passive section to enhance the modulation response of a DML by tuning the phase of the passive reflection. As indicated by the yellow line in Fig. 2(b), when the passive section phase is set as 180°, the PCG-PFL can maintain $>$35-dB SMSR for all rear facet phases. In contrast, for UG-PFL, there exists almost no front facet phase that can have good enough SMSR when the phase of HR-coated phase is between 40° to 90°.

Fig. 3 shows the time-dependent optical power distribution inside a PCG-PFL at stable and unstable conditions. Different traces indicate the power distributions at different time instances. Also shown in Fig. 3 are the corresponding optical spectrum for the stable and unstable conditions. It is clear that the power (photon) distribution in a PCG-PFL can remain very stable with good SMSR, while it fluctuates with resonant behavior when the phases cause the beating (competition) of multiple modes. Noting that the resistance to external reflection of a PCG-DFB depends on the grating length and it reaches the optimal condition with about 60% of gratings in the cavity [23], [24]. Therefore, in this work, the PCG-PFLs are designed to have 60% of gratings in the laser cavity to accomplish the greatest SMY with passive reflections [23].

Fig. 4 shows the effect of grating coupling coefficient (κ) and facet reflectivity of the passive section (R_f) on the SMY of PCG-PFLs. κ represents the strength of corrugation for the gratings and is related to the etching depth, duty cycle, and materials of the gratings [36]. By increasing the grating coupling coefficient, the SMY decreases from 85.98% for $\kappa = 8000$ m^{-1} (Fig. 2(b)) to 79.47% and 64.79% for $\kappa = 10000$ m^{-1} (Fig. 4(a)) and $\kappa = 12000$ m^{-1} (Fig. 4(b)), respectively.

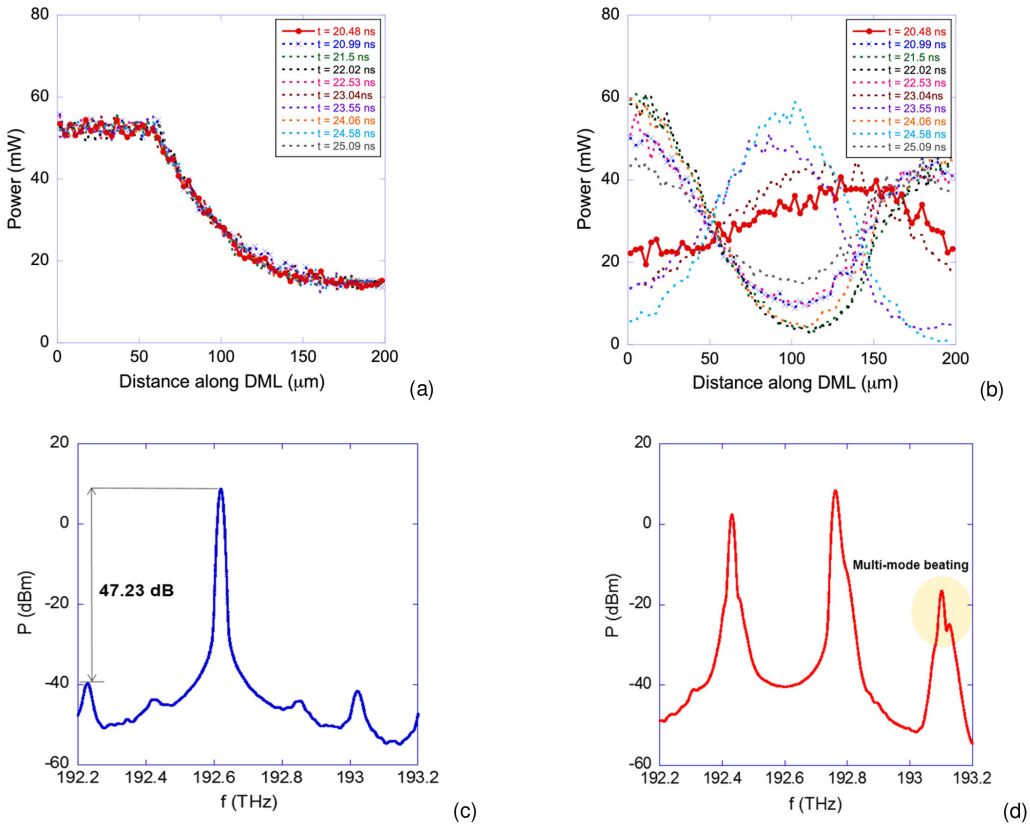

Fig. 3. Time-dependent total longitudinal power distribution of PCG-PFL at (a) stable condition (front phase = 180°), (b) unstable condition (front facet = 60°), and the corresponding optical spectrum at (c) stable and (d) unstable condition.

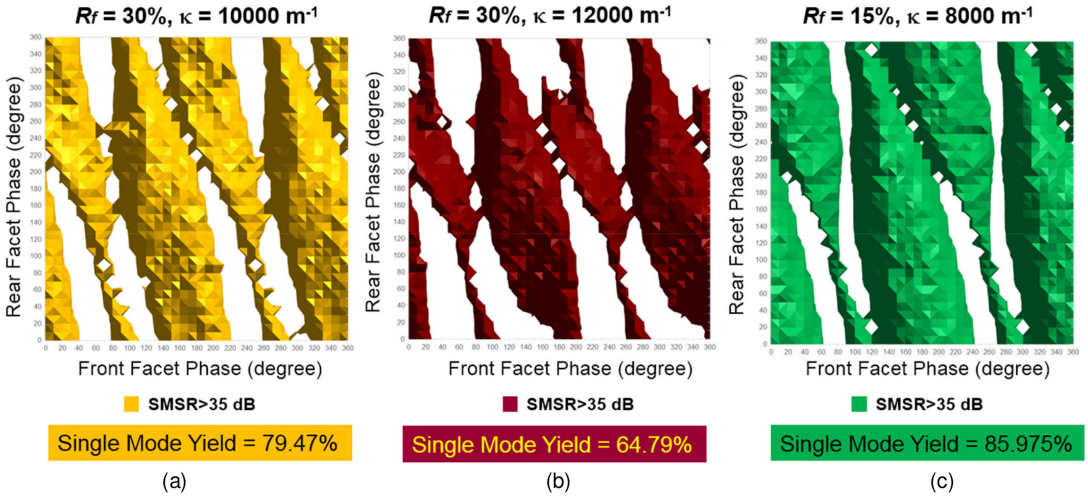

Fig. 4. SMSR versus the variation of rear facet phase and front facet phase for PCG-PFLs with different grating coupling coefficients and front facet reflectivity.

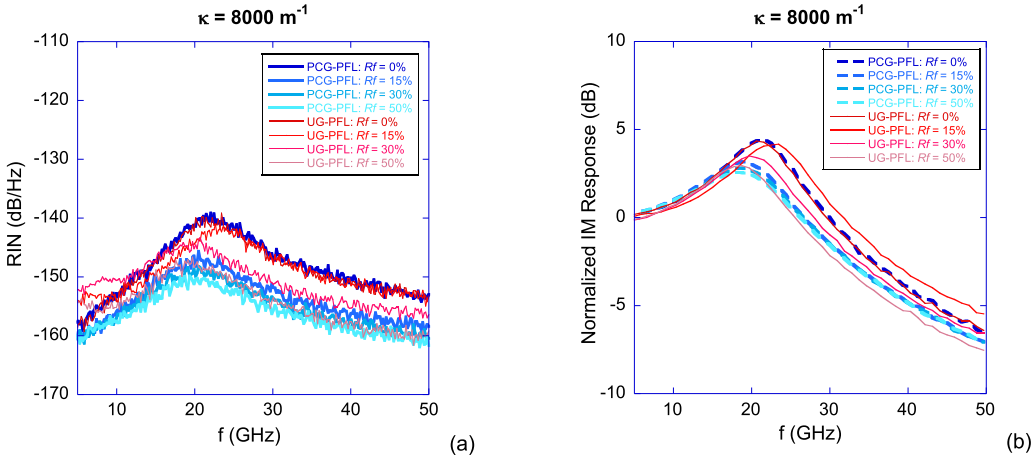

Fig. 5. (a) RIN characteristics and (b) Intensity modulation responses for PCG-PFL and UG-PFL with different residual reflections. The HR coated rear facet phase is 0° and front facet phase is 180°.

For a larger κ, the spectral bandwidth of the effective grating reflector is widened, so the difference in the mirror loss between the competing modes is usually smaller and the mode selectivity is worse. Also, the non-uniformity of the carrier and photon density distributions is more severe when a higher grating coupling coefficient is applied so that the SMSR would be reduced [47]. However, even with κ as large as 12000 m^{-1}, the SMY of PCG-PFL is still better than a UG-PFL with κ = 8000 m^{-1}. When the reflectivity from the passive reflector, R_f, is reduced to 15%, the SMY, as shown in Fig. 4(c), remains about the same as $R_f = 30\%$ though the smaller reflection case will provide a slightly higher SMSR. It is expected that, with a much larger reflection, the SMY will be degraded due to the fact that the strong feedback effect will affect the threshold condition of the lasing modes and can cause self-pulsation and mode beating [48]. With a larger tolerance on κ and R_f, the use of PCG in a PFL allows more flexible design parameters for realizing high-speed DMLs.

4.2 Improvement on RIN and Modulation Response by PCG-PFL

We have verified in Section 4.1 that the PCG-PFL can have a larger window of stable single mode operation against the phase variations in the rear (HR-coated) facet and front (passive reflector) facet. For high-speed DMLs of 100-Gb/s or above data rate, the flatness in modulation response and RIN are important performance indices in addition to the modulation bandwidth. There exist tradeoffs in the DML design to achieve the optimal performance for the targeted data rate and transmission distance. For transmitting with the modulation formats of higher spectral efficiency, like PAM-4, enough modulation bandwidth, flat modulation response, and low RIN are all very important [4], [49]. We will demonstrate the enhancement on the modulation response of a DML by a short passive feedback. On the other hand, the PPR effect is usually adopted when a lager bandwidth is needed. The design of PCG-PFL with PPR effect will also be reported.

Fig. 5 shows that the RIN and IM modulation bandwidth of a PCG-PFL with a short passive reflector decrease with the facet reflectivity. The 3-dB bandwidth is greater than 34-GHz for all the simulated passive reflection cases. The bandwidth is enough for transmitting 100-Gb/s per channel with PAM-4 modulation [4]. Noting that the responses for $R_f = 0$ corresponds to the case of PCG-DFB with a non-reflecting passive section, which was used to maintain long enough device length for short-cavity DMLs to solve the heat conduction and laser cleavage issues. The RIN and IM response for this case is the same as the short-cavity PCG-DFB. By adding a passive section with a reflectivity of 30%, the RIN and resonant peak of the IM response can be reduced by about

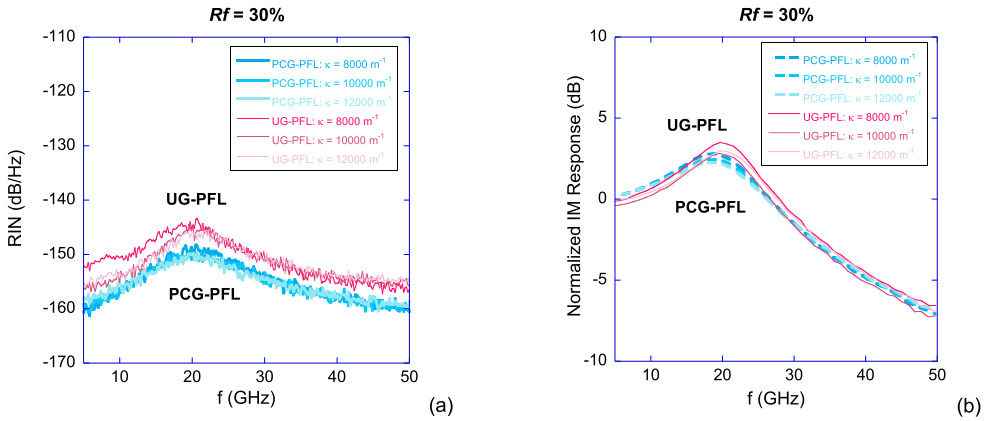

Fig. 6. (a) RIN characteristics and (b) Intensity modulation responses for PCG-PFL and UG-PFL with different grating coupling coefficient. The HR coated rear facet phase is 0° and front facet phase is 180°.

10-dB and 2-dB, respectively. The reduction in both characteristics are good for transmitting PAM-4 signals of >100-Gb/s data rates that requires a larger signal-to-noise ratio and a smaller waveform distortion. With the PCG structure, these merits from short passive reflection can be exploited without affecting the single mode stability.

The effects of optical feedback on the modulation bandwidth, resonant peak, and RIN of semiconductor lasers have been addressed in the literature [50], [51]. In general, the optical feedback can increase or decrease the bandwidth due to the change in the relaxation resonant frequency and damping factor. The sign of change depends on the phase of optical feedback. The reduction in RIN by the integrated short passive reflector is similar to the effect from optical feedback or injection locking [50], [51]. The height of resonant peak is determined by the ratio of the resonant frequency to the damping factor, which can also be modified by the passive reflection. Higher resonant peak indicates a potential larger overshoot and undershoot during upward and downward signal transitions. Though the overshoot and undershoot can be reduced by smoothing the waveform with a LPF, they still affect the waveform and eye-openings, especially for PAM-4 modulation. Our simulation results suggest that, in spite of slight reduction in modulation bandwidth, the modulation response is improved when a PCG-DFB is integrated with a reflective passive section. Such an improvement will lead to a reduced waveform distortion, which will be verified with the large signal analysis in Section 4-3.

In contrast with the effects of the passive reflector on the RIN and modulation effect, the change in grating strength barely changes the RIN spectrum and only slightly change the IM response, as shown in Fig. 6. Since $\kappa = 8000\ \mathrm{m}^{-1}$ gives a better SMY, the following analyses will be mostly based on this condition.

For comparisons, the RIN and IM responses for UG-PFL are also included in Figs. 5 and 6. UG-PFLs could have slightly larger resonance frequency but a higher resonant peak, which may result in a larger distortion in the modulation waveform. Comparing to PCG-PFLs, UG-PFLs have clearly larger RIN, which is again not good for high-speed PAM-4 modulation.

4.3 Effects on Modulation Waveforms

The reduction in resonance peak by using a PCG-PFL leads to the reduction in the over/undershoot and thus better eye diagrams, comparing to that of a PCG-DFB laser without passive section. The waveform distortion caused by the relaxation resonance is critical for PAM-4 modulation, especially when the resonant frequency is close to half-baud rate. PAM-4 signals have smaller vertical spacing between the signals levels that can fluctuate considerably as the overshoot and undershoot occurs

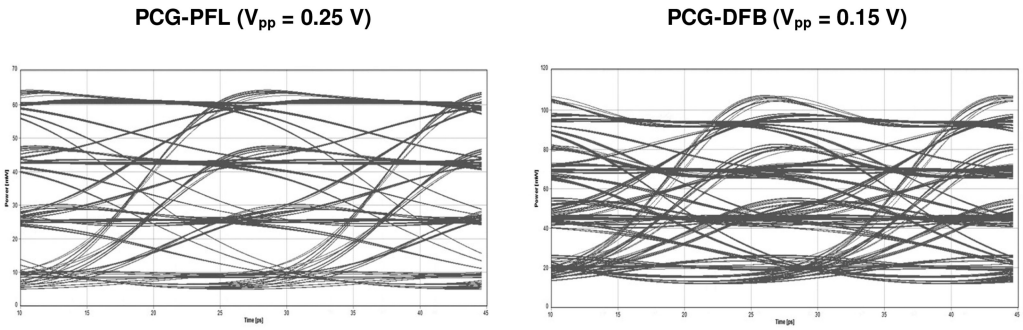

Fig. 7. Comparison of eye diagrams at 56-Gbaud/s PAM-4 signals generated by the PCG-PFL (R_f = 30%) and PCG-DFB.

during signal waveform transition. When the resonant frequency, f_r, is close to half of baud rate, the overshoot/undershoot occur near the center of the unit interval, so the eye-opening is severely degraded. This can happen for designing a high-speed DML for transmitting 56-Gbaud/s PAM-4 signals where the typical resonant frequency ranges from 20 to 30-GHz.

Fig. 7 compares the PAM-4 modulated waveforms between a PCG-DFB and a PCG-PFL with 50-μm long passive section (R_f = 30%). To make fair comparisons, a larger modulation voltage (V_{pp} = 0.25 V) is set for PCG-PFL to have about the same eye diagrams with the original PCG-DFB since the slope efficiency of the laser is reduced by adding the reflective passive section. As expected from the IM response shown in Fig. 5(b), the PCG-PFL can produce a better eye opening than the PCG-DFB laser due to the reduced overshoot and undershoot that are correlated with the reduced resonant peak. The better eye-opening results from the suppressed overshoot and undershoot by the passive reflection. It was reported both experimentally and theoretically that the optical feedback to a DFB laser caused fluctuations with the frequency of relaxation resonance on the modulated waveform [23]. This happens since the interaction between the carriers and photons is the strongest at f_r. With properly control the phase of passive reflection, the induced fluctuation can cancel part of the original relaxation resonance induced overshoot and undershoot in the modulated waveform.

From the simulation, the PCG-PFL structure with 150-μm long PCG-DFB and 50-μm long reflective passive section can generate good optical waveform for transmitting 56-Gbaud/s PAM-4 signals. The total length of 200-μm allows for easier cleavage control and better heatsink than the original 150-μm long PCG-DFB laser, but maintains nearly the same 3-dB bandwidth.

To quantitate the improvement on the optical output waveform, the simulated results for modulating a PCG-PFL and a PCG-DFB with 56-Gbaud/s PAM-4 signals are summarized in Fig. 8. The normalized eye height and overshoot/undershoot ratio, which are defined as the ratio of waveform parameters to the level spacing, are analyze for varying the phase of HR-coated rear facet. Overall, the PCG-PFL could give a better average normalized eye height of 0.699, 0.575, and 0.501 for level 1, level 2, and level 3, respectively. Though the eye diagrams are poor for the HR phase of 260° to 310°, the PCG-PFL can provide better modulation performance than a PCG-DFB over a wide range of passive reflection phase. If the optimal front facet phase is set as 180°, the PCG-PFL is able to stabilize the laser operation from the phase fluctuation of the rear facet. Hence, the PCG-PFL could maintain a small average overshoot ($<$29.23%) and a small average undershoot ($<$17.19%) than a PCG-DFB with a larger average overshoot ($<$40.09%) and larger average undershoot ($<$22.45%) throughout the rear facet variations.

4.4 PPR Effect by PCG-PFL With L_p = 200-μm

The PCG-PFL can also support PPR effect to enhance the modulation bandwidth of a DML. To move the PPR peak closer to the CPR peak, the relaxation resonance peak, a longer passive

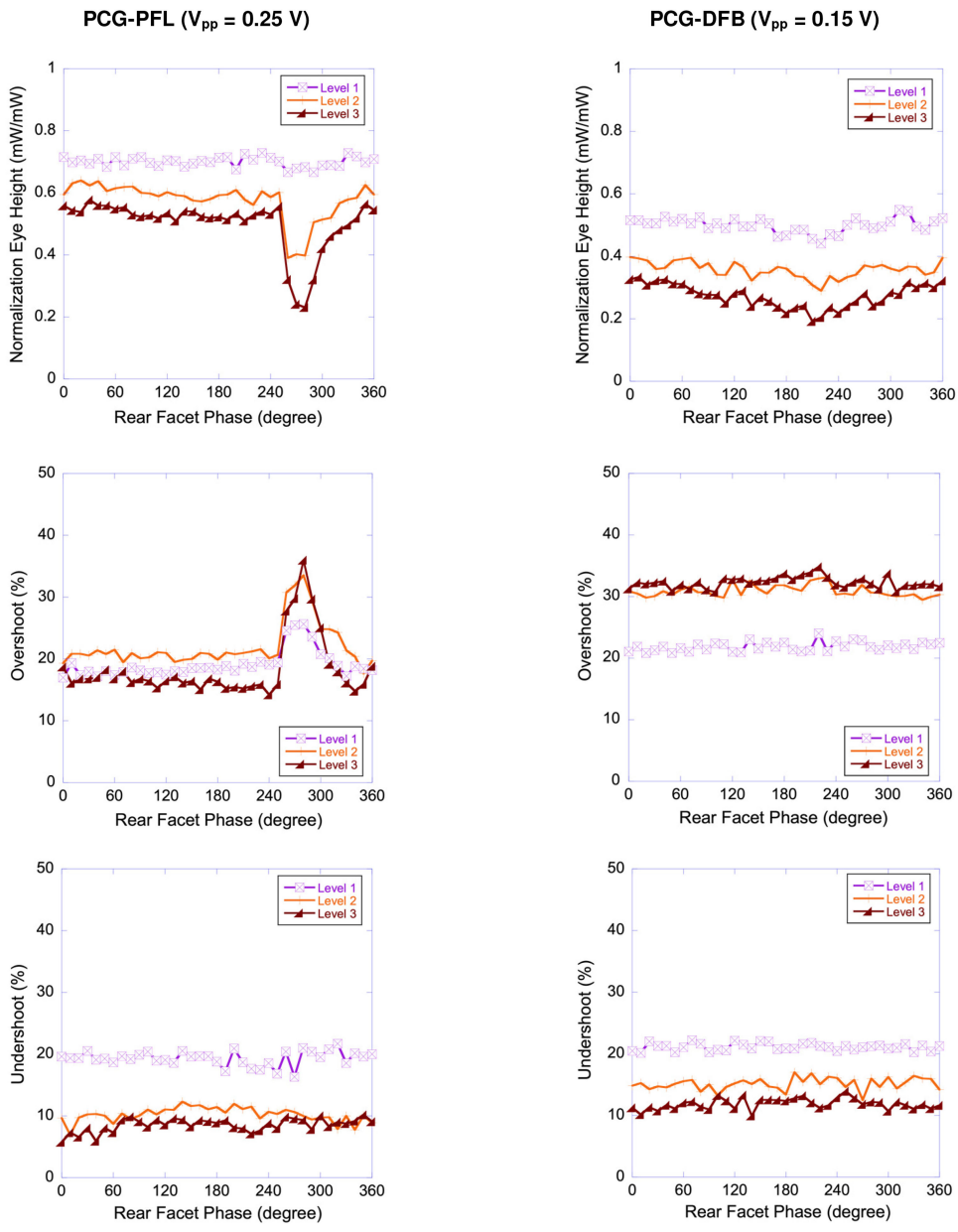

Fig. 8. Summarized results for PCG-PFL and PCG-DFB at 56-Gbaud/s PAM-4 signals (bandwidth of LPF filter = 25-GHz, front facet phase = 180°).

reflector shall be used. Fig. 9(a) shows that both CPR and PPR peaks can appear in the IM response for $L_p = 200$-μm. The IM response depends strongly on the phase of the passive reflection, so a phase tuning is needed for optimizing the flatness and bandwidth of the PPR-assisted modulation response. This enhancement is obtained by the mode interactions in the PCG-PFL [52], [53]. This PPR-assisted PCG-PFL can achieve >60-GHz 3-dB bandwidth.

The dual peaks in the IM response will lead to a larger oscillation behavior in the output waveform, which can degrade signal quality for PAM-4 modulation. Fig. 9(b) shows the simulated eye pattern under 56-Gbaud/s PAM-4 modulation for PCG-PFL with front facet phase of 60°, which has a PPR peak in the IM responses. A larger LPF filter bandwidth is used for both the transmitter and

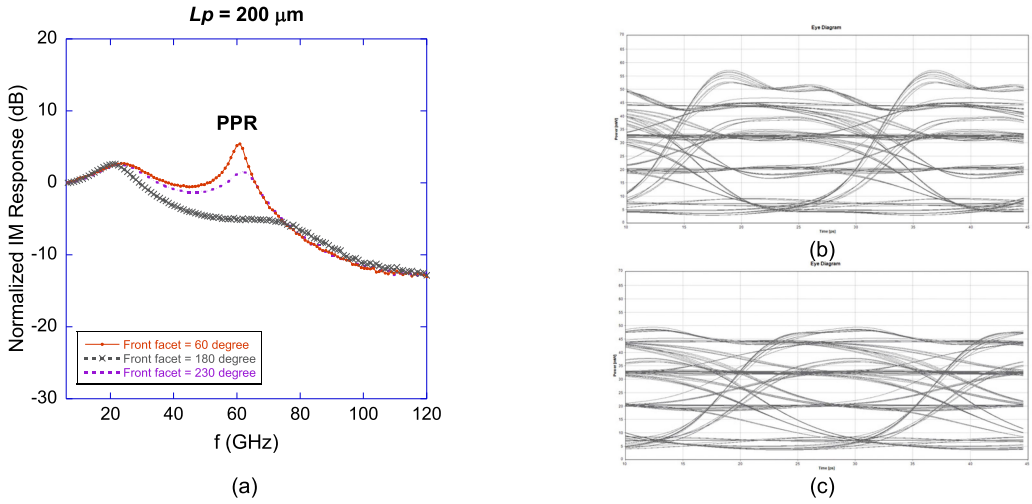

Fig. 9. (a) IM response for PCG-PFL with L_p = 200-μm and 0° HR coated rear facet phase. Eye diagrams for 56-Gbaud/s PAM-4 modulation of the PCG-PFL with (b) front facet = 60° and 56-GHz transmitter LPF and (c) front facet = 60° and 28-GHz transmitter LPF.

receiver to observe the effect of enhanced bandwidth and waveform distortion. The rise/fall time is clearly shortened due to the large bandwidth provided by the PPR effect. However, the overshoot and undershoot during the waveform transitions reduce the eye opening. It is well known that the PAM-4 modulation is very sensitive to such kind of waveform distortion and a flat IM modulation response is needed. The signal overshoot and undershoot can be suppressed by adding a LPF after the signal generator to smooth out the modulating signal, as shown in Fig. 9(c). However, eye skew can result from the low-pass filtering. The better way to overcome this problem is to optimize the PPR effect to obtain a flatter IM response.

The PPR frequency decreases as the passive section length increases. Therefore, the length, phase, and reflectivity of the passive section can be further optimized to obtain an IM modulation with a larger 3-dB bandwidth and a flatter frequency response. As pointed out in Section 2, the incorporation of PCG in the PFL allows a more flexible phase tuning and can maintain stable single-mode operation in the tuning, by comparing to a UG-PFL.

5. Conclusion

High-speed direct modulated DFB-lasers have been successfully designed by using partially corrugated grating for integration with a passive reflector to transmit >100-Gb/s signals. The use of PCG-DFB based PFLs evidently improves the operation stability of DMLs compared to conventional PFLs even with strong reflection from the passive section. This provides a robust laser structure to enhance the modulation bandwidth and/or the modulation response by integrating a passive reflector. It is also found that the PCG-PFL could reduce the RIN and resonant peak, which enhance the waveform and eye opening for high-speed PAM-4 modulation. Furthermore, an ultrahigh modulation bandwidth could be achieved with PPR effect by integration of a PCG-DFB with a mid-length passive reflector.

For a PCG-PFL with 150-μm laser section, 50-μm passive section, HR-coated rear facet, and 30% front-facet reflectivity, the simulation indicated a single-mode yield as high as 85.98% when κ = 8000 m^{-1}. With a front facet phase 180°, the PCG-PFL can maintain >35-dB SMSR irrespective of the rear HR coating phase. Such a PCG-PFL can produce a good 3-dB bandwidth (>34-GHz), and the passive feedback helps to reduce the RIN and resonant peak of the IM response by about 10-dB and 2-dB, respectively. This PCG-PFL can generate good optical

waveform for transmitting 56-Gbaud/s PAM-4 signals. The better eye-opening results from the reduced overshoot ($<$29.23%) and undershoot ($<$17.19%) by the passive reflection. The 200-μm long total device length allows for easier cleavage control and better heatsink than the original 150-μm long PCG-DFB laser, while the 3-dB bandwidth is nearly the same.

The integrated passive section in a PCG-PFL can also be designed to exploit the PPR effect to enhance the modulation bandwidth of a DML. A PCG-PFL with 200-μm long passive reflector is designed to have a PPR peak closer to the relaxation resonance peak of the PCG-DFB laser and display $>$60-GHz 3-dB bandwidth. The incorporation of PCG in the PFL provides a robust structure to allow further optimization of the length, phase, and reflectivity of the passive section so as to obtain an IM modulation with a larger 3-dB bandwidth and a flat frequency response.

References

[1] K. Naoe, T. Nakajima, Y. Nakai, Y. Yamaguchi, Y. Sakuma, and N. Sasada, "Advanced InP laser technologies for 400G and beyond hyperscale interconnections," in *Proc. SPIE Photon. Europe Conf.*, 2020, Art. no. 1135604.

[2] K. Nakahara *et al.*, "112-Gb/s PAM-4 uncooled (25 °C to 85 °C) directly modulation of 1.3-μm InGaAlAs-MQW DFB BH lasers with record high bandwidth," in *Proc. 45th ECOC*, 2019, Art. no. PD.2.4.

[3] N. Sasada *et al.*, "Wide-temperature-range (25–80 °C) 53-Gbaud PAM4 (106-Gb/s) operation of 1.3-μm directly modulated DFB lasers for 10-km transmission," *J. Lightw. Technol.*, vol. 37, no. 7, pp. 1686–1689, 2019.

[4] F. Zhu, Y. Wen, and Y. Bai, "Component BW requirement of 56Gbaud modulations for 400GbE 2 & 10 km PMD," in *Proc. IEEE 802.3bs 400GbE Task Force Plenary Meeting*, 2014, pp. 1–13.

[5] A. Laakso and M. Dumitrescu, "Modified rate equation model including the photon-photon resonance," in *Proc. NUSOD*, 2010, Art. no. ThB3.

[6] N. H. Zhu *et al.*, "Directly modulated semiconductor lasers," *IEEE J. Sel. Topics Quantum Electron.*, vol. 24, no. 1, pp. 1–19, Jan./Feb. 2017.

[7] E. K. Lau, X. Zhao, H. K. Sung, D. Parekh, C. C. Hasnain, and M. C. Wu, "Strong optical injection-locked semiconductor lasers demonstrating $>$100-GHz resonance frequencies and 80-GHz intrinsic bandwidths," *Opt. Exp.*, vol. 16, no. 9, pp. 6609–6618, 2008.

[8] O. Kjebon, R. Schatz, S. Lourdudoss, S. Nilsson, B. Stalnacke, and L. Backbom, "30 GHz direct modulation bandwidth in detuned loaded InGaAsP DBR lasers at 1.55 μm wavelength," *Electron. Lett.*, vol. 33, no. 6, pp. 486–489, 1997.

[9] Y. Matsui *et al.*, "55 GHz bandwidth distributed reflector laser," *J. Lightw. Technol.*, vol. 35, no. 3, pp. 397–403, 2017.

[10] G. Liu, G. Zhao, J. Sun, D. Gao, Q. Lu, and W. Guo, "Experimental demonstration of DFB lasers with active distributed reflector," *Opt. Exp.*, vol. 26, no. 23, pp. 29784–29795, 2018.

[11] K. Otsubo *et al.*, "AlGaInAs quantum-well lasers with semi-insulating buried-heterostructure for high-speed direct modulation up to 40 Gbps," in *Proc. SPIE-OSA-IEEE Asia Comm. Photon.*, 2009, Art. no. 76311Q.

[12] J. Kreissl, V. Vercesi, U. Troppenz, T. Gaertner, W. Wenisch, and M. Schell, "Up to 40 Gb/s directly modulated laser operating at low driving current: Buried-heterostructure passive feedback laser (BH-PFL)," *IEEE Photon. Technol. Lett.*, vol. 24, no. 5, pp. 362–364, Mar. 2012.

[13] M. Radziunas *et al.*, "Improving the modulation bandwidth in semiconductor lasers by passive feedback," *IEEE J. Sel. Topics Quantum Electron.*, vol. 13, no. 1, pp. 136–142, Jan./Feb. 2007.

[14] O. V. Ushakov, S. Bauer, O. Brox, H. J. J. Wunsche, and F. Henneberger, "Dynamics of lasers with ultrashort optical feedback," in *Proc. Integrate. Optolectron. Dev.*, 2004, Art. no. 5349.

[15] O. Ozolins *et al.*, "100 GHz externally modulated laser for optical interconnects," *J. Lightw. Technol.*, vol. 35, no. 6, pp. 1174–1179, 2017.

[16] G. Morthier *et al.*, "High-speed directly modulated heterogeneously integrated Inp/Si DFB laser," in *Proc. ECOC*, 2016, Art. no. M.2.E.1.

[17] J. Li *et al.*, "Monolithically integrated multi-section semiconductor lasers: Towards the future of integrated microwave photonics," *Inter. J. Light Elect. Optic.*, vol. 226, no. 165724, pp. 1–29, 2020.

[18] N. P. Diamantopoulos *et al.*, "$>$100-GHz bandwidth directly-modulated lasers and adaptive entropy loading for energy-efficient $>$300-Gbps/λ IM/DD systems," *J. Lightw. Technol.*, vol. 39, no. 3, pp. 771–778, Feb. 2021.

[19] N. P. Diamantopoulos *et al.*, "Net 321.24-Gb/s IMDD transmission based on a $>$100-GHz bandwidth directly-modulated laser," in *Proc. OFC*, 2020, Art. no. Th4C.1.

[20] Y. Huang, T. Okuda, K. Shiba, and T. Torikai, "High-yield external optical feedback resistant partially-corrugated-waveguide laser diodes," in *Proc. IEEE 16th Int. Semicond. Laser Conf.*, 1998, Art. no. TuE44.

[21] M. Gotoda, T. Nishimura, K. Matsumoto, T. Aoyagi, and K. Yoshiara, "Highly external optical feedback tolerant 1.49 μm single-mode lasers with partially corrugated gratings," in *Proc. IEEE 21st Int. Semicond. Laser Conf.*, 2008, Art. no. MB8.

[22] K. Zhong *et al.*, "Experimental study of PAM-4, CAP-16, and DMT for 100 Gb/s short reach optical transmission systems," *Opt. Exp.*, vol. 23, no. 2, pp. 1176–1189, 2015.

[23] Y. Huang, T. Okuda, K. Shiba, Y. Muroya, N. Suzuki, and K. Kobayashi, "External optical feedback resistant 2,5-Gb/s transmission of partially corrugated waveguide laser diodes over a $-$40 °C to 80 °C temperature range," *IEEE Photon. Technol. Lett.*, vol. 11, no. 11, pp. 1482–1484, 1999.

[24] P. D. Pukhrambam, S. L. Lee, and G. Keiser, "Electroabsorption modulated lasers with immunity to residual facet reflection by using lasers with partially corrugated gratings," *IEEE Photon. J.*, vol. 9, no. 2, Apr. 2017, Art. no. 7101016.

[25] S. Mieda, N. Yokota, R. Isshiki, W. Kobayashi, and H. Yasaka, "Frequency response control of semiconductor laser using hybrid modulation scheme," *Opt. Exp.*, vol. 24, no. 22, pp. 25824–25831, 2016.
[26] T. Tadokoro, W. Kobayashi, T. Fujisawa, T. Yamanaka, and F. Kano, "High-speed modulation lasers for 100GbE applications," in *Proc. Opt. Fiber Comm. Conf.*, 2011, Art. no. OWD1.
[27] M. Shirao, K. Kojima, and H. Itamoto, "53.2 Gb/s NRZ transmission over 10 km using high-speed EML for 400 GbE," in *Proc. Opto-Electron. Comm. Conf.*, 2015, Art. no. JThC.22.
[28] Y. Nakai *et al.*, "Uncooled operation of 53-GBd PAM4 (106-Gb/s) EA-DFB lasers with extremely low drive voltage with 0.9 vpp," *J. Lightw. Technol.*, vol. 37, no. 7, pp. 1658–1662, 2019.
[29] C. Bornholdt *et al.*, "40 Gbit/s directly modulated passive feedback DFB laser for transmission over 320 km single mode fibre," in *Proc. 34th ECOC*, 2008, Art. no. Tu.1.D.6.
[30] J. Ohtsubo, *Semiconductor Lasers*, 1st ed., Verlag, Berlin: Springer, 2017.
[31] J. L. Beylat and J. Jacquet, "Analysis of DFB semiconductor lasers with external optical feedback," *Electron. Lett.*, vol. 24, no. 9, pp. 509–510, 1988.
[32] M. F. Alam, M. A. Karim, and S. Islam, "Analysis of external optical feedback characteristics of asymmetric, quarter-wave-shifted, distributed-feedback semiconductor lasers," *App. Opt.*, vol. 36, no. 18, pp. 4131–4137, 1997.
[33] O. Brox *et al.*, "High-frequency pulsations in DFB lasers with amplified feedback," *IEEE J. Quantum Electron.*, vol. 39, no. 11, pp. 1381–1387, Nov. 2003.
[34] L. A. Coldren, S. W. Corzine, and M. L. Masanovic, *Diode Laser and Photonics Integrated Circuits*, 2nd ed., Hoboken, NJ, USA: Wiley, 2012.
[35] U. Troppenz *et al.*, "40 Gbit/s directly modulated lasers: Physics and application," in *Proc. SPIE OPTO Conf.*, 2011, Art. no. 79530F.
[36] *VPIcomponentMaker 10.0 Photonic Circuit User's Manual*. Somerset, NJ, USA: VPIsystems Inc., 2019.
[37] A. Lowery *et al.*, "Multiple signal representation simulation of photonic devices, systems, and networks," *IEEE J. Sel. Topics Quantum Electron.*, vol. 6, no. 2, pp. 282–296, Mar./Apr. 2000.
[38] G. Morthier and B. Moeyersoon, "Intensity noise and linewidth of laser diodes with integrated semiconductor optical amplifier," *IEEE Photon. Technol. Lett.*, vol. 14, no. 12, pp. 1644–1646, Dec. 2002.
[39] W. Zhao *et al.*, "Modulation bandwidth enhancement of monolithically integrated mutually coupled distributed feedback laser," *App. Sci.*, vol. 10, no. 4375, pp. 1–13, 2020.
[40] A. J. Lowery, "New dynamic multimode model for external cavity semiconductor lasers," *IEE Proc. J. Optoelectron.*, vol. 136, no. 4, pp. 229–237, 1989.
[41] L. Hairong and H. G. Shiraz, "Applications of the transmission line laser model in analysis of multiple-phase-shift DFB lasers," *Microw. Opt. Technol. Lett.*, vol. 40, no. 1, pp. 51–57, 2004.
[42] Y. Matsui, H. Murai, S. Arahira, Y. Ogawa, and A. Suzuki, "Novel design scheme for high-speed MQW lasers with enhanced differential gain and reduced carrier transport effect," *IEEE J. Quantum Electron.*, vol. 34, no. 12, pp. 2340–2349, Dec. 1998.
[43] S. Sulikhah, H. W. Tsao, and S. L. Lee, "Enhancement of modulation responses of directly modulated lasers with passive feedback and partially corrugated grating," in *Proc. 24th Microoptics Conf.*, 2019, Art. no. G-3.
[44] Y. C. Lu *et al.*, "Improved SPM tolerance and cost-effective phase modulation duobinary transmission over 230 km standard single-mode fiber using a single Mach-Zender modulator," *IEEE Photon. Technol. Lett.*, vol. 17, no. 12, pp. 2754–2756, Dec. 2005.
[45] H. Venghaus and N. Grote, *Fibre Optic Communication*, 2nd ed., Berlin, Germany: Springer, 2017.
[46] G. Katz and E. Sonkin, "Level optimization of PAM-4 transmission with signal-dependent noise," *IEEE Photon. J.*, vol. 11, no. 1, Feb. 2019, Art. no. 7200606.
[47] H. Virtanen, T. Uusitalo, and M. Dumitrescu, "Simulation studies of DFB laser longitudinal structures for narrow linewidth emission," *Optic. Quant. Electron.*, vol. 49, no. 160, pp. 1–13, 2017.
[48] M. M. Bouchene and R. Hamdi, "The effect of facets reflectivity on the static characteristics of (DFB) semiconductor laser," in *Proc. CISTEM*, 2018, Art. no. 202.
[49] Y. G. Zhao *et al.*, "High-power and low-noise DFB semiconductor lasers for RF photonic links," in *Proc. IEEE Avi., Fiber-Opt. Photon. Dig. CD*, 2012, Art. no. WD3.
[50] G. P. Agrawal and N. K. Dutta, *Semiconductor Lasers*, 2nd ed., Van Nostrand R., Ed., New York, NY, USA: Van Nostrand Reinhold, 1993.
[51] M. F. Ferreira, J. F. Rocha, and J. L. Pinto, "FP and DFB semiconductor lasers with arbitrary external optical feedback," in *Proc. SPIE OE/FIBERS*, 1989, pp. 33–44.
[52] M. Dumitrescu, T. Uusitalo, H. Virtanen, A. Laakso, P. Bardella, and I. Montrosset, "Simulation of photon-photon resonance enhanced direct modulation bandwidth of DFB lasers," in *Proc. NUSOD*, 2016, Art. no. TuP12.
[53] T. Uusitalo, H. Virtanen, P. Bardella, and M. Dumitrescu, "Analysis of the photon-photon resonance influence on the direct modulation bandwidth of dual-longitudinal-mode distributed feedback lasers," *Optic. Quant. Electron.*, vol. 49, no. 46, pp. 1–4, 2017.